5-1-2017

# Analysis of Beam Deflection Measurements in the Presence of Linear Absorption

Manuel R. Ferdinandus
*Air Force Institute of Technology*

Jennifer Reed
*Air Force Research Laboratory*

Kent L. Averett

F. Kenneth Hopkins

Augustine Urbas
*Air Force Research Laboratory*



## Recommended Citation

Manuel R. Ferdinandus, Jennifer M. Reed, Kent L. Averett, F. Kenneth Hopkins, and Augustine Urbas, "Analysis of beam deflection measurements in the presence of linear absorption," Opt. Mater. Express 7, 1598-1605 (2017). https://doi.org/10.1364/OME.7.001598

Research Article | Vol. 7, No. 5 | 1 May 2017 | OPTICAL MATERIALS EXPRESS 1598

Optical Materials EXPRESS

# Analysis of beam deflection measurements in the presence of linear absorption

MANUEL R. FERDINANDUS,[1,*] JENNIFER M. REED,[2] KENT L. AVERETT, F. KENNETH HOPKINS, AND AUGUSTINE URBAS[2]

[1]*Department of Engineering Physics, Air Force Institute of Technology, 2950 Hobson Way, Wright-Patterson AFB, OH 45433, USA*
[2]*Materials and Manufacturing Directorate, Air Force Research Laboratory, 5135 Pearson Road, Wright-Patterson AFB, OH 45433, USA*
**manuel.ferdinandus@us.af.mil*

**Abstract:** We develop a series of analytical approximations allowing for rapid extraction of the nonlinear parameters from beam deflection measurements. We then apply these approximations to the analysis of cadmium silicon phosphide and compare the results against previously published parameter extraction methods and find good agreement for typical experimental conditions.



**OCIS codes:** (190.4400) Nonlinear optics, materials; (190.3270) Kerr effect.

## References and links

1. D. N. Christodoulides, I. C. Khoo, G. J. Salamo, G. I. Stegeman, and E. W. Van Stryland, "Nonlinear refraction and absorption: mechanisms and magnitudes," Adv. Opt. Photonics **2**(1), 60–200 (2010).
2. C. B. de Araújo, A. S. L. Gomes, and G. Boudebs, "Techniques for nonlinear optical characterization of materials: a review," Rep. Prog. Phys. **79**(3), 036401 (2016).
3. J. K. Wahlstrand, J. H. Odhner, E. T. McCole, Y. H. Cheng, J. P. Palastro, R. J. Levis, and H. M. Milchberg, "Effect of two-beam coupling in strong-field optical pump-probe experiments," Phys. Rev. A **87**(5), 053801 (2013).
4. B. A. Ruzicka, S. Wang, J. Liu, K.-P. Loh, J. Z. Wu, and H. Zhao, "Spatially resolved pump-probe study of single-layer graphene produced by chemical vapor deposition [Invited]," Opt. Mater. Express **2**(6), 708–716 (2012).
5. E. Dremetsika, B. Dlubak, S. P. Gorza, C. Ciret, M. B. Martin, S. Hofmann, P. Seneor, D. Dolfi, S. Massar, P. Emplit, and P. Kockaert, "Measuring the nonlinear refractive index of graphene using the optical Kerr effect method," Opt. Lett. **41**(14), 3281–3284 (2016).
6. D. S. Kummli, H. M. Frey, and S. Leutwyler, "Femtosecond degenerate four-wave mixing of carbon disulfide: high-accuracy rotational constants," J. Chem. Phys. **124**(14), 144307 (2006).
7. M. R. Ferdinandus, H. Hu, M. Reichert, D. J. Hagan, and E. W. Van Stryland, "Beam deflection measurement of time and polarization resolved ultrafast nonlinear refraction," Opt. Lett. **38**(18), 3518–3521 (2013).
8. R. A. Negres, J. M. Hales, A. Kobyakov, D. J. Hagan, and E. W. Van Stryland, "Experiment and analysis of two-photon absorption spectroscopy using a white-light continuum probe," Quantum Electronics, IEEE Journal of **38**(9), 1205–1216 (2002).
9. M. Reichert, H. Hu, M. R. Ferdinandus, M. Seidel, P. Zhao, T. R. Ensley, D. Peceli, J. M. Reed, D. A. Fishman, S. Webster, D. J. Hagan, and E. W. Van Stryland, "Temporal, spectral, and polarization dependence of the nonlinear optical response of carbon disulfide," Optica **1**(6), 436 (2014).
10. G. V. Naik, V. M. Shalaev, and A. Boltasseva, "Alternative plasmonic materials: beyond gold and silver," Adv. Mater. **25**(24), 3264–3294 (2013).
11. G. Wang, S. Zhang, X. Zhang, L. Zhang, Y. Cheng, D. Fox, H. Zhang, J. N. Coleman, W. J. Blau, and J. Wang, "Tunable nonlinear refractive index of two-dimensional $MoS_2$, $WS_2$, and $MoSe_2$ nanosheet dispersions [Invited]," Photonics Research **3**(2), A51 (2015).
12. K. J. A. Ooi, J. L. Cheng, J. E. Sipe, L. K. Ang, and D. T. H. Tan, "Ultrafast, broadband, and configurable midinfrared all-optical switching in nonlinear graphene plasmonic waveguides," APL Photonics **1**(4), 046101 (2016).
13. M. Reichert, P. Zhao, J. M. Reed, T. R. Ensley, D. J. Hagan, and E. W. Van Stryland, "Beam deflection measurement of bound-electronic and rotational nonlinear refraction in molecular gases," Opt. Express **23**(17), 22224–22237 (2015).
14. M. R. Ferdinandus, H. Hu, M. Reichert, Z. Wang, D. J. Hagan, and E. Van Stryland, "Beam deflection measurement of time and polarization resolved nonlinear refraction," in *Frontiers in Optics 2013*, I. R. D. A. N. Kang, and D. Hagan, eds. (Optical Society of America, Orlando, Florida, 2013), p. FTh4C.2.

#286316 https://doi.org/10.1364/OME.7.001598
Journal © 2017 Received 7 Feb 2017; revised 30 Mar 2017; accepted 30 Mar 2017; published 12 Apr 2017

Optical Materials EXPRESS

15. N. Kinsey, A. A. Syed, D. Courtwright, C. DeVault, C. E. Bonner, V. I. Gavrilenko, V. M. Shalaev, D. J. Hagan, E. W. Van Stryland, and A. Boltasseva, "Effective third-order nonlinearities in metallic refractory titanium nitride thin films," Opt. Mater. Express **5**(11), 2395 (2015).
16. S. C. Kumar, M. Jelínek, M. Baudisch, K. T. Zawilski, P. G. Schunemann, V. Kubeček, J. Biegert, and M. Ebrahim-Zadeh, "Tunable, high-energy, mid-infrared, picosecond optical parametric generator based on $CdSiP_2$," Opt. Express **20**(14), 15703–15709 (2012).
17. V. Kemlin, B. Boulanger, V. Petrov, P. Segonds, B. Ménaert, P. G. Schunneman, and K. T. Zawilski, "Nonlinear, dispersive, and phase-matching properties of the new chalcopyrite $CdSiP_2$ [Invited]," Opt. Mater. Express **1**(7), 1292–1300 (2011).
18. K. T. Zawilski, P. G. Schunemann, T. C. Pollak, D. E. Zelmon, N. C. Fernelius, and F. Kenneth Hopkins, "Growth and characterization of large $CdSiP_2$ single crystals," J. Cryst. Growth **312**(8), 1127–1132 (2010).
19. K. Kato, N. Umemura, and V. Petrov, "Sellmeier and thermo-optic dispersion formulas for $CdSiP_2$," J. Appl. Phys. **109**(11), 116104 (2011).
20. G. Ghosh, "Sellmeier coefficients for the birefringence and refractive indices of $ZnGeP_2$ nonlinear crystal at different temperatures," Appl. Opt. **37**(7), 1205–1212 (1998).
21. S. Chaitanya Kumar, J. Krauth, A. Steinmann, K. T. Zawilski, P. G. Schunemann, H. Giessen, and M. Ebrahim-Zadeh, "High-power femtosecond mid-infrared optical parametric oscillator at 7 μm based on $CdSiP_2$," Opt. Lett. **40**(7), 1398–1401 (2015).
22. S. C. Kumar, M. Jelínek, M. Baudisch, K. T. Zawilski, P. G. Schunemann, V. Kubeček, J. Biegert, and M. Ebrahim-Zadeh, "Tunable, high-energy, mid-infrared, picosecond optical parametric generator based on $CdSiP_2$," Opt. Express **20**(14), 15703–15709 (2012).

## Introduction

Knowledge of the temporal response of the Nonlinear Refraction (NLR) and Nonlinear Absorption (NLA) of materials is key for understanding of the physical mechanisms underlying the Nonlinear Optical (NLO) properties [1]. Various experimental techniques have been developed for measuring this response [2]. Commonly used methods such as pump – probe [3, 4] provide the temporal response of the NLA, the refraction via the induced birefringence as in the Optical Kerr Effect (OKE) experiment [5] or with use of a local oscillator as with four wave mixing [6]. The Beam Deflection (BD) method was developed as a high sensitivity, easy to implement time and polarization resolved technique for simultaneous measurement of NLR and NLA [7].

Previously, techniques for analyzing BD data for instantaneous and non-instantaneous nonlinearities in the presence of Group Velocity Mismatch (GVM) have been determined [8, 9]. This method, however is limited in that it only treats materials in the undepleted excitation approximation, where the absorption is sufficiently small so that irradiance throughout the sample is constant. This is a significant limitation, especially in probing 2-D, plasmonic and metamaterials which typically have high linear and nonlinear absorption [10, 11]. These materials have come to be of interest to the NLO community for a variety of application such as photonic-electronic interconnects, all optical switching and computing and hybrid silicon photonics [12].

Additionally, depending on the spatial and temporal resolution required, this method can be very time consuming and makes the extraction of NLO parameters tedious, especially for materials with multiple mechanisms acting together. In this work we develop an analytic approach that accounts for change in the excitation throughout the sample due to linear, absorption. To demonstrate the validity of these approximations, we will compare them against previous extraction methods to show good agreement for typical experimental conditions. We then apply our approximations to measurements of Cadmium Silicon Phosphide (CSP), a material with large index dispersion and linear absorption.

## 1. Analysis of beam deflection data

The BD method operates by using a strong Gaussian excitation beam to generate an index change $\Delta n$ within the material as seen in Fig. 1. If the spot size of the probe is much smaller than the excitation, the probe, displaced from the peak by half the beam waist of the excitation, experiences a prism-like index gradient. This transient prism deflects the beam by some angle $\Delta\theta$. This deflection angle is in turn in measured by the quadrant cell diode as a

Optical Materials EXPRESS

change in the differential energy signal of the probe $\Delta E_p[\tau_d] = E_{p,L} - E_{p,R,}$ where $E_{p,(L,R)}$ are the probe signal measured from the left and right sides of the quadrant diode and $\tau_d$ is the delay between the excitation and probe. This signal is normalized by the total energy of the probe $E_p[\tau_d] = E_{p,L} + E_{p,R}$ so that the signal $\Delta E_p / E_p[\tau_d]$ is proportional to $\Delta n$ [13]. Similarly, the NLA can be extracted using total energy signal $E_p[\tau_d]$ which can be normalized to calculate the transmission.

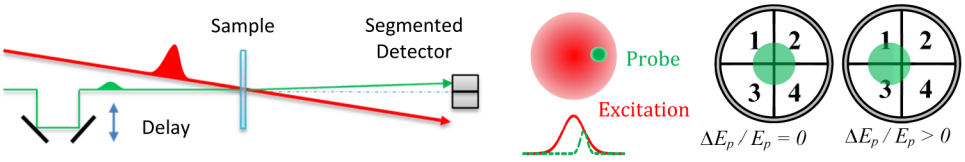


Fig. 1. Schematic of the beam deflection experiment with the probe displaced at $\Delta x = w_e / 2$. Diagram of the irradiance profiles of the excitation and probe pulses. When the probe is centered on the quad-segmented photodiode the signal $\Delta E_p / E_p = 0$, when deflected $\Delta E_p / E_p > 0$.

Following the method outlined in Reichert et al [9], we start with the propagation equation in the absence of Group Velocity Dispersion (GVD) in normalized coordinates.

$$\frac{\partial a_p[\boldsymbol{r},Z,\tau]}{\partial Z} + \rho \frac{\partial a_p[\boldsymbol{r},Z,\tau]}{\partial \tau} = \left(-\sigma_p + iG[\boldsymbol{r},Z,\tau]\right) a_p[\boldsymbol{r},Z,\tau] \tag{1}$$

where $a_p[\boldsymbol{r},Z,t]$ is the dimensionless field of the probe, $Z = z / L$ is the normalized propagation distance, $L$ is the sample length, $\tau = t / \tau_e$ is the normalized temporal coordinate, $\tau_e$ is the excitation pulse duration $\sigma_p = \alpha_p L / 2$ is the normalized linear absorption of the probe, $\rho = \Delta n_g L / (\tau_e c)$ is the GVM parameter, $\Delta n_g$ is the difference in the group indices of the excitation and probe, $c$ is the speed of light in vacuum and $\alpha_p$ is the linear absorption of the probe. $G[\boldsymbol{r},Z,\tau] = \int_{-\infty}^{\infty} R[\tau - \tau'] \left|a_e[\boldsymbol{r},Z,\tau]\right|^2 d\tau'$ is the convolution of the nonlinear response function $R[\tau] = (\eta + i\Gamma) r[\tau]$ and the dimensionless excitation irradiance $|a_e[\boldsymbol{r},Z,\tau]|^2$. The response function $r[\tau]$ is normalized such that $\int_{-\infty}^{\infty} r[\tau] d\tau = 1$. The dimensionless nonlinear refraction and absorption parameters are $\eta = (4\pi / \lambda_p) n_2 I_{0,e} L$ and $\Gamma = \alpha_2 I_{0,e} L$ where $\lambda_p$ is the probe wavelength, $n_2$ is the nonlinear index of refraction, $I_{0,e}$ is the peak irradiance of the excitation and $\alpha_2$ is the nonlinear absorption coefficient. For bandwidth limited Gaussian spatiotemporal profiles we have

$$a_e[\boldsymbol{r},Z,\tau] = e^{-\left((X-X_0)^2+Y^2\right)} e^{-\tau^2/2} e^{-Z\sigma_e} \tag{2}$$

$$a_p[\boldsymbol{r},0,\tau] = A e^{-\left(\frac{X^2+Y^2}{W^2}\right)} e^{-\frac{(\tau-\tau_d)^2}{2T^2}} \tag{3}$$

where $a_e[\boldsymbol{r},Z,\tau]$ is the field of the excitation, shifted so the probe is centered over the maximum gradient of the spatial envelope ($X_0 = ½$), $a_p[\boldsymbol{r},0,\tau]$ is the field of the probe at the front of the sample, and $X = x / w_e$, $Y = y / w_e$ are the normalized spatial coordinates, $\sigma_e = \alpha_e L / 2$ is the normalized linear absorption parameter of the excitation, $\alpha_e$ is the linear absorption of the excitation, $T = \tau_p / \tau_e$ is the ratio of the pulse durations, $W = w_{0,p} / w_e$ is the ratio of the spot sizes of the beams, and $w_{0,p}$ and $w_e$ are the $1 / e^2$ spot sizes of the probe and excitation. We can solve for the field at the back of the sample $a_p[\boldsymbol{r},1,\tau]$ in the linear ($L << z_{0,p}$) and nonlinear ($L << z_{0,p} / \Delta\varphi_0$) thin sample approximations where $z_{0,p}$ is the Rayleigh range of the probe and $\Delta\varphi_0$ is the peak induced phase shift. Typically, $\Delta\varphi_0 << 1$ and $L$ can be selected to meet these conditions giving us

Optical Materials EXPRESS

$$a_p[r,1,\tau] = A \cdot Exp\left[ -\left( \frac{X^2+Y^2}{W^2} \right) - \frac{(\rho-\tau+\tau_d)^2}{2T^2} - \sigma_p - e^{-2(X-X_0)^2-2Y^2} H[\tau] \right] \quad (4)$$

$$H[\tau] = \int_1^0 \left( iG[0,Z',\tau+\rho(-1+Z')] \right) dZ' = H'[\tau] + iH''[\tau] \quad (5)$$

where $H[\tau]$ is the integral for the pulse overlap in the sample accounting for GVM and depletion of the excitation due to linear absorption. The real part $H'[\tau]$ corresponds to the change in the absorption $\Delta\alpha_p$ and $H''[\tau]$ corresponds to the nonlinear phase accumulation $\Delta\varphi_p$. As in previous work the signal can be calculated by Fresnel propagating $a_p[\boldsymbol{r},1,\tau]$ and spatially integrating over both sides of the detector and temporally over the pulse duration. In this analysis we use the convenience that the Fresnel propagation to the detector will yield another Gaussian expanded in size, deflected by an angle $\Delta\theta$ due to $H''[\tau]$ and attenuated due to $H'[\tau]$.

The complex transmission $t[\boldsymbol{r},\tau]$ applied to the probe by the material response induced by the excitation is $t[\boldsymbol{r},\tau] = Q[\boldsymbol{r},\tau]\mathrm{Exp}[i\varphi[\boldsymbol{r},\tau]]$. If $W$ is sufficiently small ($W << 1$) and the deflection is small ($\Delta\theta << 1$) we can expand the magnitude and phase transmissions as

$$\begin{aligned} Q[r,\tau] &= e^{-2e^{-2\left((X-X_0)^2+Y^2\right)}H'[\tau]} \\ &\approx \sum_0^\infty 2^n \left( -e^{-2X_0^2} H'[\tau] \right)^n \left( 1 - 8e^{-2X_0^2} XX_0 H'[\tau] \right) / n! \end{aligned} \quad (6)$$

$$\phi[r,\tau] = \mathrm{Tan}\left[ e^{-2(X-X_0)^2-2Y^2} H''[\tau] \right] \approx e^{-2(X-X_0)^2-2Y^2} H''[\tau] \quad (7)$$

As shown in Fig. 2, the effect of this attenuation is to make it appear as if the probe beam has been translated slightly, without distorting its shape significantly. Thus while $\varphi[\boldsymbol{r},\tau]$ acts as the prism that deflects the probe an angle $\Delta\theta$, $Q[\boldsymbol{r},\tau]$ attenuates and slightly translates the probe yielding a small deflection signal due to NLA.

The average deflection angle of the probe is $\Delta\theta[\tau] = 4e^{-2X_0^2} X_0 H''[\tau] R / \left( k_{0,p} w_e \right)$, where $R = e^{2X_0^2 - 2X_0^2/(1+2W^2)} / \left( 1+2W^2 \right)^2$. With $Q[\boldsymbol{r},\tau]$ and $\Delta\theta[\tau]$ we can use Gaussian beam propagation instead of Fresnel propagation to calculate the probe field at the detector a normalized distance $D = d / z_{0,p}$ away from the sample

$$\begin{aligned} &a_d[\boldsymbol{r},\tau,\tau_d] = \\ &\sum_{n=0}^\infty \frac{2^n A^2 e^{-\frac{2Y^2}{D^2W^2} - \frac{2(X-\Delta S[\tau])^2}{D^2W^2} - \frac{(\rho-\tau+\tau_d)^2}{T^2}} \left( -e^{-2X_0^2} H'[\tau] \right)^n \left( 1 + 8e^{-2X_0^2} X_0 \left( -X + \Delta S[\tau] \right) H'[\tau] \right)}{D^2 n!} \end{aligned} \quad (8)$$

where $\Delta S[\tau] = \Delta\theta[\tau] d / w_e$ is the normalized lateral beam displacement on the detector due to the deflection and $d$ is the sample – detector distance. Integrating and then re-summing the probe irradiance $|a_d[\boldsymbol{r}, \tau, \tau_d]|^2$ we calculate the difference in the power between the left and right sides $\Delta P[\tau, \tau_d]$ and the total power $P[\tau, \tau_d]$

Optical Materials EXPRESS

$$\Delta P\left[\tau,\tau_d\right]=2A^2e^{-2X_0^2-\frac{\left(\rho-\tau+\tau_d\right)^2}{T^2}-2e^{-2X_0^2}H'[\tau]}\sqrt{2\pi}W^3X_0\left(RH''\left[\tau\right]+H'\left[\tau\right]/D\right) \tag{9}$$

$$P\left[\tau,\tau_d\right]=\frac{1}{2}A^2e^{-\frac{(\rho-\tau+\tau_d)^2}{T^2}-\frac{2H'[\tau]}{\sqrt{e}}}\pi W^2 \tag{10}$$

To calculate $\Delta E_p[\tau_d]$ and $E_p[\tau_d]$ we integrate $\Delta P[\tau,\tau_d]$ and $P[\tau,\tau_d]$ over $\tau$, which we then divide to yield the normalized signal $\Delta E_p$ / $E_p[\tau_d]$. The transmission $Q[\tau_d]$ is calculated by normalizing $E_p[\tau_d]$ by its value at some large negative delay. Because this calculation does not involve performing Fresnel propagation at every time $\tau$ and delay $\tau_d$, this method an order of magnitude faster, allowing for automated parameter fitting.

For an instantaneous response ($r[t] = \delta[t]$) with negligible GVM ($\rho = 0$) the overlap integrals reduce to $H'[\tau]=\Gamma e^{-\tau^2}F$ and $H''[\tau]=\eta e^{-\tau^2}F$, where $F$ is the attenuation factor accounting for the linear absorption of the excitation. For beam deflection ($X_0 = ½$), $\Delta P[\tau,\tau_d]$ and $P[\tau,\tau_d]$ can be integrated over $\tau$ analytically so that an expression can be found for $\Delta E_p$ / $E_p[\tau_d]$,

$$\Delta E_p\,/\,E_p\left[\tau_d\right]=\frac{2e^{-\frac{1}{2}-\frac{\tau_d^2}{1+T^2}}\sqrt{\frac{2}{\pi}}W\left(\Gamma/D+R\eta\right)}{\sqrt{T^2+1}}F \tag{11}$$

$$F=-\frac{-1+e^{-2\sigma_e}}{2\sigma_e} \tag{12}$$

In the case of no linear absorption ($\sigma_e = 0$, $F \to 1$), excitation much larger than the probe ($W << 1$, $R \to 1$), and negligible NLA ($\Gamma \approx 0$), Eq. (11) reduces to the previously derived expression for the signal in transparent material [14]. Note that by setting $X_0 = 0$, Eq. (10) can be used to calculate the expression for the transmission in excite – probe experiments [8]

$$Q\left[\tau_d\right]=\frac{1}{\sqrt{\pi}T}\int_{-\infty}^{\infty}e^{-\frac{(\rho-\tau+\tau_d)^2}{T^2}-2H'[\tau]}d\tau \tag{13}$$

Taking the ratio of the deflection signal due to the refraction ($\Delta E_p$ / $E_p[\Gamma = 0]$) and absorption ($\Delta E_p$ / $E_p[\eta = 0]$) we define the contamination factor $C = (\Delta E_p$ / $E_p[\eta = 0])$ / $(\Delta E_p$ / $E_p[\Gamma = 0])$ $\propto 1 / D$. As we seen in Fig. 2 the effect of a small translation is reduced by the expansion of the probe as it propagates to the detector, while the translation due to the deflection scales with distance. For a typical configuration ($D > 15$) we can effectively set $H'[\tau] = 0$ in Eq. (9). This makes the BD method particularly well suited for measuring materials with large NLA since the refraction and absorption signals are essentially independent of each other. This approach has been applied to BD measurements of thin film refractory metal nitrides, which possess both high linear and nonlinear absorption [15].

Optical Materials EXPRESS

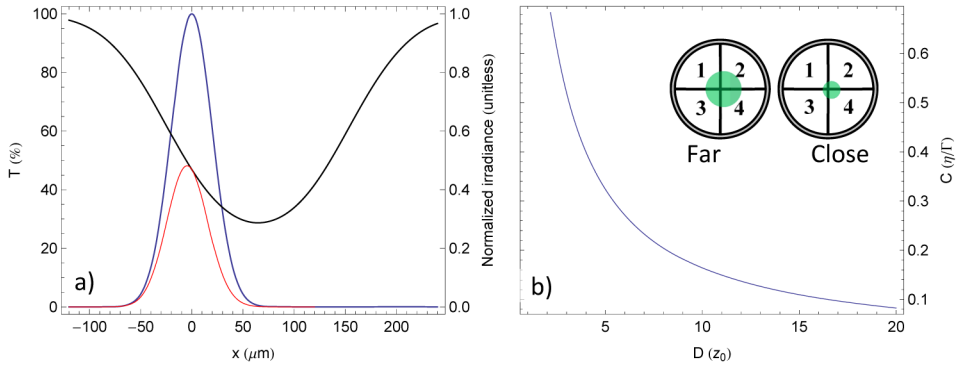


Fig. 2. a) Effect of magnitude transmission gradient on probe beam. For $W << 1$ the transmission gradient (black) makes it appear as if probe (blue) has been reduced in magnitude and translated with minimal distortion (red). b) Plot of contamination $C$ for vs. normalized sample-detector distance $D$. For typical experimental geometries ($D > 15$), $C << 1$, so that the NLA and NLR signals are essentially independent. b inset) For small $D$ the probe is small on the detector, so that a translation has a large effect of $\Delta E_p$. For $D >> 1$, $\Delta E_p$ due to the same translation is much smaller due to the expansion of the beam over the increased propagation distance.

## 2. Comparisons to previous models

In Fig. 3 we compare the method from Reichert et al and our analysis for various values of $\rho$, along with our approximations compared to the Fresnel propagation method. The agreement between the Fresnel propagation and the analytical expression is very good, with a difference at the peak signal of less than 2.0%.

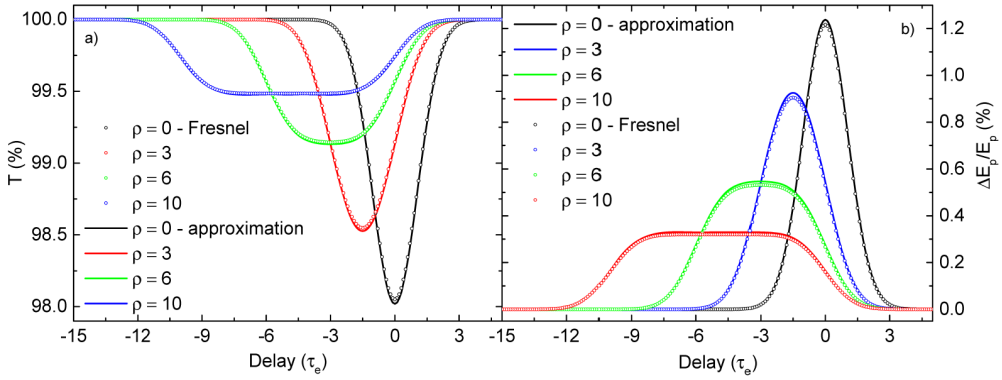


Fig. 3. Comparison of Fresnel propagation (open circles) and analytical method (solid lines) for various values of $\rho$ with $\sigma_e = 0$ for the a) transmission and b) deflection. The analytical method shows excellent agreement, with an error of less than 2.0% at the peak of the signal. The simulation parameters are $W = 0.175$, $T = 1.09$, $\eta = 0.118$, $\Gamma = 0$, $D = 16.78$ with $\rho$ variable.

As seen in Fig. 4, the effect of GVM is to extend the temporal range of the signal, as one would expect as it is possible for the excitation pulse to walk entirely through the probe pulse over a wide range of delays [8]. The effect of the excitation depletion is to reduce the signal at negative delays due to the excitation catching up to the probe at the back of the sample after it has been significantly attenuated.

Optical Materials EXPRESS

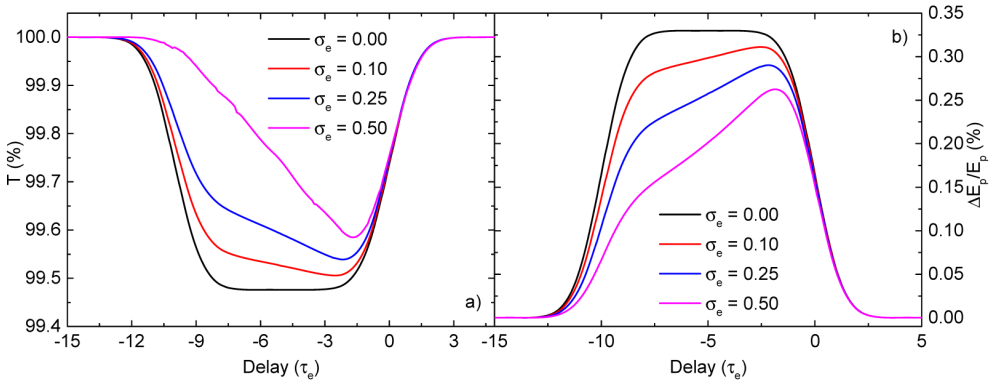


Fig. 4. a) Transmission and b) refraction signals for various values of linear absorption $\sigma_e$ with $\rho = 10$. The simulation parameters are $W = 0.175$, $T = 1.09$, $\eta = 0.118$, $\Gamma = 0$, $D = 16.78$ with $\sigma_e$ variable. Increasing $\sigma_e$ reduces the signal at negative delay due to the excitation catching up to the probe at the back of sample, after it has been attenuated by propagation through the sample.

## 3. Measurements of cadmium silicon phosphide

To test the validity of our analysis, we fit measurements of CSP using both the above expressions. CSP is a II-IV-$V_2$ chalcopyrite semiconductor with a high 2nd order nonlinear coefficient ($d_{36}$) of 84.5 pm/V in the mid-infrared spectrum [16] with sufficient birefringence for 2 μm to mid-IR wavelength conversion [17]. Grown by the horizontal gradient freeze technique, CSP shows significantly improved transparency (i.e., lower optical absorption), unfortunately combined with a somewhat lower thermal conductivity, as compared to the more established Zinc Germanium Phosphide (ZGP) [18]. These properties suggest that CSP will display a higher thermal-lensing threshold and thus enable higher power mid-IR laser output than possible with ZGP [19, 20]. Previous works have demonstrated CSP based high power femtosecond Optical Parametric Amplifiers (OPA) pumped at 1064 nm [21].

BD measurements are made using a Ti:Sapphire amplified system (KM Labs Wyvern 1000-10) producing 4.2 mJ, 35 fs (FWHM) pulses at 790 nm operating at a 1 kHz repetition rate. The strong excitation pulse is obtained by splitting off ~5 μJ of the fundamental with a beam splitter. An optical parametric generator/amplifier (Light Conversion TOPAS-Prime) is pumped by the fundamental to generate the 650 nm, 55 fs probe pulses, which is then spatially filtered to produce a Gaussian irradiance profile. The probe is focused to a spot size, $w_p$ ~3 – 5 times smaller than $w_e$, both which were determined by knife-edge scans. The probe is displaced from the peak of the excitation by $\Delta x = ½w_e$ to the maximized irradiance gradient where the probe experiences an induced refractive index gradient, causing it to be deflected by a small angle $\Delta\theta$. The deflection signal is measured using a quad-segmented Si photodiode (OSI QD50-0-SD) which simultaneously measures $\Delta E_p[\tau_d]$ and $E_p[\tau_d]$, each of which is detected via lock-in detection (Stanford Systems SR-830). A mechanical optical chopper (Thorlabs MC-2000) synchronized with the excitation repetition rate is used to modulate the excitation at 286 Hz.

Optical Materials EXPRESS

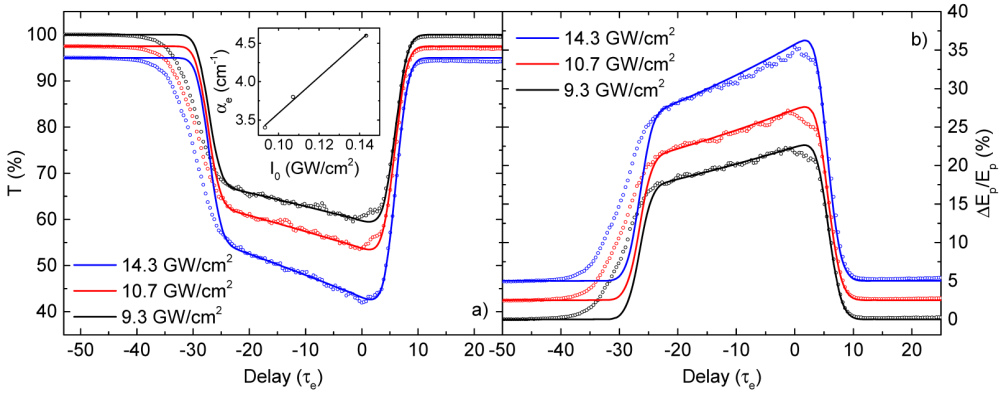


Fig. 5. Fit of CSP data using analytic approximation for a) transmission and b) deflection. Note that the reduction in the signal between $\tau_d$ = 5 and $\tau_d$ = 25 is due to the depletion of the excitation. The difference in the slope of the rise and fall of the signal is due to GVD, which is not accounted for. Inset) absorption coefficient $\alpha_e$ vs. peak excitation irradiance $I_{0,e}$. Plots have been shifted vertically by 2.5% for clarity.

Figure 5 shows measurements of CSP at $\lambda_p$ = 650 nm and $\lambda_e$ = 800 nm. Using the expressions Eq. (9) – 10 we fit values for the nondegenerate parameters $n_2$ = 115 x $10^{-19}$ m$^2$/W and $\alpha_2$ = 8.8 x $10^{-11}$ m/W, with $\rho$ = 33 and values of $\alpha_e$ as shown in the inset of Fig. 5 a). The increase in the linear absorption of the excitation as a function of irradiance follows the form of an effective 2PA of the excitation modeled as $\alpha_e[I] = \alpha_0 + \alpha_{2,e}I$. Fitting the data we find an linear absorption coefficient $\alpha_0$ = 1.22 cm$^{-1}$ and an effective 2PA coefficient of $\alpha_{2,e}$ = 0.23 x $10^{-11}$ m/W. The extracted nonlinear parameters are on the same order ($\alpha_2$ = 2.4 x $10^{-11}$ m/W) as previously reported degenerate measurements at 1 µm [22]. The deviation of the fit from the data at negative delay is due to the GVD, which broadens the pulses as they propagate through the material, thus reducing the irradiance and the induced nonlinear effect. This effect is not modeled in order to derive an analytic solution for Eq. (1). It may be possible to determine the GVD either through ellipsometry measurements or by BD measurements of differing thicknesses of material.

## 4. Conclusions

We have extended the analysis of BD data to include depletion of the excitation due to linear absorption. Additionally, we have applied a series of approximations in order to arrive at analytic expressions that are much quicker to evaluate than the standard Fresnel propagation based methods. We have shown that the approximations have very good agreement with the Fresnel propagation method, with a difference of less than 2%. Lastly we have applied these expressions to the extraction of the nonlinear properties of CSP.